Table 2. Depth scaling factors for the open and blocked field and relative electron densities of commercially available solid phantoms. The depth scaling factors are determined from photon energy spectra at 10 cm depth for 10 cm × 10 cm open and blocked field, respectively.

Phantom	$(\rho_e)_{pl,w}$	Nominal photon energy [MV]							
		4		6		10		15	
		Open	*MBF	Open	MBF	Open	MBF	Open	MBF
WT1	0.972	0.971	0.970	0.970	0.969	0.967	0.966	0.964	0.965
457-CTG	0.972	0.971	0.970	0.970	0.969	0.967	0.966	0.964	0.965
RW3	0.966	0.965	0.964	0.964	0.962	0.958	0.957	0.953	0.954
MixDP	1.012	1.010	1.009	1.008	1.006	1.001	1.000	0.996	0.997
WE211	0.973	0.972	0.972	0.971	0.970	0.968	0.967	0.965	0.966
WE211R	0.974	0.974	0.973	0.973	0.972	0.969	0.969	0.966	0.967
Plastic Water	0.969	0.970	0.970	0.970	0.970	0.970	0.970	0.970	0.970
Plastic Water DT	0.963	0.963	0.963	0.962	0.962	0.962	0.962	0.961	0.961
Virtual Water	0.968	0.968	0.967	0.967	0.966	0.963	0.963	0.961	0.961
Polystyrene	0.969	0.967	0.966	0.965	0.963	0.958	0.957	0.953	0.954
PMMA	0.972	0.970	0.970	0.969	0.968	0.965	0.965	0.963	0.963
ABS	0.972	0.970	0.969	0.968	0.966	0.961	0.960	0.956	0.957

*MBF : MLC blocked field

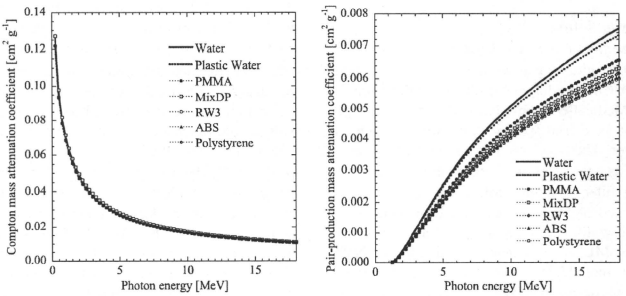

(a) (b)

Fig. 1. (a) Compton mass attenuation coefficients and (b) pair-production mass attenuation coefficients for several solid phantoms.[16]

mined from the effective mass attenuation coefficient.

Depth and field size dependence

Figure 2 shows simulated photon energy spectra in water at various depths (a) on beam central axis for 10 MV photon beam with various size of open field (b) as an example of simulation results. Each spectrum was normalized to total photon fluence of the sampling region. E_{av} shows average photon energy determined from the photon spectrum.

As depth increase, photon energy was hardened by attenuation with a medium. The contribution of scattered photon was increased and E_{av} was decreased with increasing field size. Therefore, the beam hardening effect on the spectrum became small for large field.

Table 3 shows the depth scaling factors of the polystyrene for various depths and field sizes because it shows large

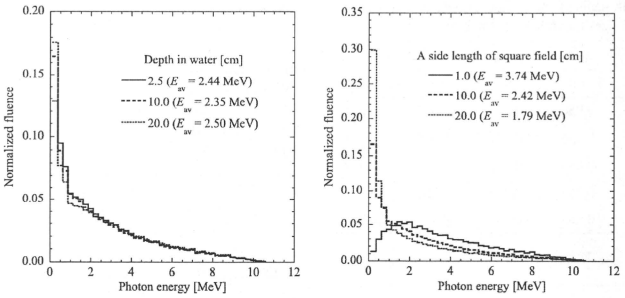

Fig. 2. Photon energy spectra in water for the 10 MV photon beam as a function of (a) depth and (b) field size at 10 cm depth. The each spectrum is normalized to total fluence of the sampling region. E_{av} shows average photon energies for each photon spectrum.

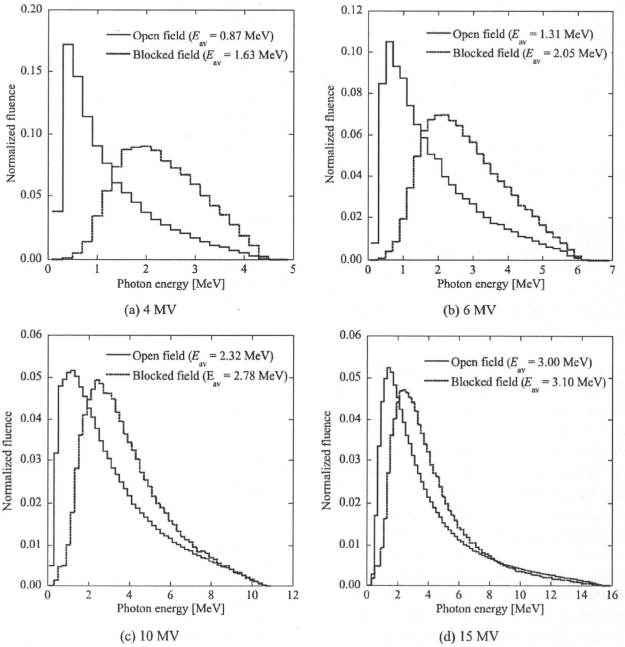

Fig. 3. Photon energy spectra in 2 cmϕ central area at phantom surface for the open field and blocked field for (a) 4 MV, (b) 6 MV, (c) 10 MV and (d) 15 MV. The each spectrum was normalized to total fluence of the sampling region.

Table 3. Depth scaling factors of the polystyrene for various depths and field sizes for 10 MV photon beam.

Depth [cm]	A side length of square field [cm]			
	1.0	5.0	10.0	20.0
2.5	0.956	0.957	0.958	0.958
5.0	0.956	0.957	0.958	0.958
10.0	0.955	0.957	0.958	0.958
15.0	0.955	0.956	0.957	0.958
20.0	0.954	0.955	0.957	0.958

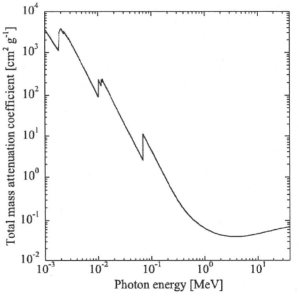

Fig. 4. The total mass attenuation coefficient for tungsten.[9]

photon energy dependency. As mentioned above, the depth scaling factor is strongly depending on proportion of high energy part in the spectrum. The proportion of high energy part was constant even though depth and field size were changed, consequently, depth scaling factors were almost constant.

Influence of beam hardening effect by the MLC

Photon energy spectra at a phantom surface for open field and blocked field with the same jaw setting, 10 cm × 10 cm, are shown in Fig. 3. For all photon energies, the lower energy photons were removed by the MLC which tungsten has high mass attenuation coefficient for low energy photons as shown in Fig. 4. Furthermore, for 15 MV beam, reduction of high energy photons was also observed because tungsten has minimum mass attenuation coefficient at 4 MeV and the mass attenuation coefficient increases above 4 MeV.

The depth scaling factors for blocked field with 10 cm × 10 cm jaw setting are also tabulated in Table 2. For the Plastic Water, the depth scaling factor for the blocked field was equal to that of open field. On the other hand, the depth scaling factor of the RW3, MixDP, polystyrene, PMMA and ABS for the blocked field were obviously different from the relative electron densities. For the polystyrene, the difference of z_{pl} scaled by the relative electron density becomes 2.0 mm at 10 cm depth. This is because pair-production mass attenuation coefficients of these solid phantoms are different from water. However, the depth scaling factor for the blocked field was almost equal to the depth scaling factor for the open field. The z_{pl} determined from both scaling factors agreed within 0.2 mm at 10 cm depth.

Consequently, to minimize the error of the depth scaling for IMRT beams, the depth scaling factor should be obtained from the effective mass attenuation coefficient.

Conclusion

To clarify the accurate depth scaling method for IMRT beam, the variations of photon energy spectra for various radiation fields and depth scaling factors were determined. The results clarified that the depth scaling factor of Plastic Water were independent on photon energy. On the other hand, the depth scaling factors of the other phantoms were significantly different by photon energy. Therefore depth must be scaled by using presented depth scaling factor corresponding to photon beam energy.

The results also clarified that the ratio of effective mass attenuation coefficients of media to water are unaffected by whether open or blocked field. The presented depth scaling factor can also be used for IMRT beams.

In the future, this study can be used to clarify the effect of spectral variation for fluence scaling.

REFERENCES

1. Seuntjens J, *et al* (2005) Absorbed dose to water reference dosimetry using solid phantoms in the context of absorbed-dose protocols. Med Phys **32**: 2945–2953.
2. IAEA (2004) Absorbed Dose Determination in External Beam Radiotherapy: An International Code of Practice for Dosimetry Based on Standards of Absorbed Dose to Water. TRS 398. pp. 39–41. International Atomic Energy Agency, Vienna.
3. Pruitt JS and Loevinger R (1982) The photon-fluence scaling theorem for Compton-scattered radiation. Med Phys **9**: 176–179.
4. Onai Y and Kusumoto G (1959) Trial Production of a Water-Equivalent Solid Phantom Material. JJR **19**: 1012–1016. (in Japanese)
5. JSMP (2002) Standard Dosimetry of Absorbed Dose in External Beam Radiotherapy (Standard Dosimetry 01). pp. 165–172, Tsusho Sangyo Kenkyu Sha; Tokyo. (in Japanese)
6. Olivares M, *et al* (2001) Electron fluence correction factors for various materials in clinical electron beams. Med Phys **28**: 1727–1734.
7. Araki F, *et al* (2009) Monte Carlo calculations of correction factors for plastic phantoms in clinical photon and electron beam dosimetry. Med Phys **36**: 2992–3001.
8. Hine GJ (1952) The effective atomic numbers of materials for various gamma ray processes. Phys Rev **85**: 725.
9. Hubbell JH (1969) Photon Cross Sections, Attenuation Coef-

ficients and Energy Absorption Coefficients from 10 keV to 100 GeV. Natl Stand Ref Data Ser **29**.
10. Rogers DW, *et al* (1995) BEAM: a Monte Carlo code to simulation radiotherapy treatment units. Med Phys **22**: 503–524.
11. Heath E and Seuntjens J (2003) Development and validation of a BEAMnrc component module for accurate Monte Carlo modeling of the Varian dynamic Millennium multileaf collimator. Phys Med Biol **48**: 4045–4063.
12. AAPM (2001) Basic applications of multileaf collimators. AAPM Report No 72. pp. 9–10. Medical Physics Publishing, Wisconsin.
13. Sheikh-Bagheri D and Rogers DW (2002) Sensitivity of megavoltage photon beam Monte Carlo simulations to electron beam and other parameter. Med Phys **29**: 379–390.
14. Tzedakis A, *et al* (2004) Influence of initial electron beam parameters on Monte Carlo calculated absorbed dose distributions for radiotherapy photon beams. Med Phys **31**: 907–913.
15. Rogers DWO, *et al* (2000) NRC User Codes for EGSnrc. NRCC Report PIRS-702. pp. 64–68. National Research Council of Canada, Ottawa.
16. Berger MJ, *et al* (2005) XCOM: Photon Cross Section Database (version 1.3). [Online] Available: http://physics.nist.gov/xcom [2010, July 14]. National Institute of Standards and Technology, Gaithersburg, MD.

Received on May 13, 2010
Revision received on August 10, 2010
Accepted on September 2, 2010
J-STAGE Advance Publication Date: October 20, 2010